

## Article

# Robust Superhydrophobic Coatings for Enhanced Corrosion Resistance and Dielectric Properties

Wentao Shao <sup>1</sup>, Qi Kan <sup>2,3</sup>, Xinxin Bai <sup>1</sup> and Chengqian Wang <sup>1,\*</sup><sup>1</sup> The 58th Research Institute of China Electronics Technology Group Corporation, Wuxi 214072, China<sup>2</sup> AVIC Aerodynamics Research Institute, Shenyang 110034, China<sup>3</sup> Aviation Key Laboratory of Science and Technology on High Speed and High Reynolds Number Aerodynamic Force Research, Shenyang 110034, China

\* Correspondence: chengqiankk@yeah.net

**Abstract:** Multifunctional super-repellent composite coatings play an important part in academic and industrial fields, while it is still a great challenge to effectively integrate a variety of functions into one material. Mg alloys having low density, high strength-to-weight ratio, and good shielding, are widely used in electronic devices, while it is susceptible to severe corrosion especially in moist air and ocean atmosphere. Here, a versatile superhydrophobic coating with organic-inorganic hybrid structure and hierarchical surface textures, integrating robust wettability with design manipulation is synthesized by assembling modified SiO<sub>2</sub> nanoparticles on polytetrafluoroethylene (PTFE) layer on the AZ31 Mg alloy. The composite coating has good water repellency with a contact angle of 170.5°, due to the micro/nano textures and low surface energy. The composite coating increases the corrosion potential of AZ31 Mg from −1.483 V to −1.243 V, and reduces the corrosion current density by 3 orders of magnitude. Remarkably, the superhydrophobic coating displays enticing damage-resistance (>40 cycles), superior environmental stability (thermal shock and outdoor placement) and self-cleaning function. Moreover, the composite coatings display excellent electrical properties with superior voltage resistance (>30 V/μm), and high resistivity (>10<sup>12</sup> Ω·cm), as well the coating has a low dielectric constant (≈3.91) and dielectric loss (0.0094), which are great advantages for the electronic or electrical engineering applications. We expect that the versatile super-repellent coating can be used as candidates for novel advanced energy materials, especially in harsh environments.

**Keywords:** Mg alloy; functional coating; robust superhydrophobicity; corrosion resistance; dielectric properties



**Citation:** Shao, W.; Kan, Q.; Bai, X.; Wang, C. Robust Superhydrophobic Coatings for Enhanced Corrosion Resistance and Dielectric Properties. *Coatings* **2022**, *12*, 1655. <https://doi.org/10.3390/coatings12111655>

Academic Editor: Saleema Noormohammed

Received: 20 September 2022

Accepted: 25 October 2022

Published: 31 October 2022

**Publisher's Note:** MDPI stays neutral with regard to jurisdictional claims in published maps and institutional affiliations.



**Copyright:** © 2022 by the authors. Licensee MDPI, Basel, Switzerland. This article is an open access article distributed under the terms and conditions of the Creative Commons Attribution (CC BY) license (<https://creativecommons.org/licenses/by/4.0/>).

## 1. Introduction

In the information age, more attention has been paid to the stability and accuracy of electronic devices in communication transmission [1]. Among them, the carrier carrying electronic components and its connection lines play an indispensable role. Generally, carrier materials [2–5] need to have high electrical insulation to meet the insulation shielding of current conduction, strong weather resistance to adapt to the complex external environment (such as natural rain falling, sunshine irradiation and wind blowing), light weight and easy to form.

Magnesium alloy has always been an attractive candidate material in the aerospace and electronics industry owing to its unmatched performances such as low density, high ductility, excellent thermal conductivity and electrical conductivity [6–11]. However, magnesium alloy is susceptible to severe damage when used in harsh environments due to its chemical reactivity, which severely limits its application [12–14]. Moreover, magnesium alloys cannot be used in high-voltage circumstances, due to having no electrical insulating property. As is well known, the transmission function of the communication device is also affected by rainfall, which tends to accumulate on the device surface to form a thin

water film, finally resulting in a reduction of transmission accuracy and a loss increment. Surface treatments to prepare MgO coating [15–18] are essential for improving the performance of magnesium alloy and elongating its service-life, while the MgO coating surface is hydrophilic with limited performance improvements.

Recently, super water-repellent surface with a water contact angle over  $150^\circ$  has remarkable properties and strong comprehensive superiority, which is considered to be one of the most prospective surface treatments for magnesium alloys [19–22]. Hence, it is necessary to design a superhydrophobic coating with a wide operating temperature range, superior weather resistance and anti-fouling. Furthermore, it needs to be endowed with multifunctional features of high electrical insulating property and excellent corrosion resistance.

According to nature bionics, superhydrophobicity is the main feature of evolutionary adaption following natural features, which is achieved through low-surface-energy chemicals and exploiting micro/nanoscale structure [23–25]. Artificial superhydrophobic coatings were designed and fabricated on magnesium by means including etching technique [26,27], spray [28,29], sol-gel method [30], electrodeposition [31–33] and template syntheses [34]. Nevertheless, the special wettability of these superhydrophobic coatings is vulnerable to damage under rigorous and complex physical/chemical settings because of the inherent fragility of micro/nano grading structure, resulting in reduced service life and limited application fields in many cases.

Additionally, unlike the extensive development of superhydrophobic coatings, the multi-functionalization with electrical properties and heavy anti-corrosion has not been fully utilized, which may broaden the application of superhydrophobic coatings in novel electronic devices fields [35]. Especially with the rapid development of modern technology, the demand for magnesium alloys is becoming more and more changeable, and a single performance has been unable to cope with new and strict challenges. At the same time, for instance, magnesium alloys are used as radar support plate or support, tail cabin body, surface coating materials for radar protection need not only good protective properties in complex environments, but also good dielectric properties, including low dielectric constant and low dielectric loss tangent. The purpose is to make the equipment antenna have large transmittance (power transmission coefficient), low reflectivity and loss, and high insulation, so as to meet the requirements of radar search and aiming accuracy on the basis of protecting radar. However, the effective integration of a variety of functions (super-hydrophobic, corrosion resistance and electrical properties, etc.) remains a major challenge. Another major challenge with superhydrophobic materials operating harsh environment is the mismatch between ambient temperature and hydrophobicity, where most water-repellent materials are prone to failure in high-temperature applications, which is the common problem.

Herein, we proposed a feasible strategy to fabricate a robust superhydrophobic composite coating by assembling modified  $\text{SiO}_2$  nanoparticles on PTFE layer, for the protection of electronic devices in harsh environments based on organic and inorganic hybridization. The relationship between surface morphology and wettability is discussed. The corrosion resistance of different coatings and Mg alloy substrate was characterized by potentiodynamic polarization curves, and the corrosion protection mechanism was revealed. The appropriate organic-inorganic network structures and hierarchical surface textures give the composite coating with durable water repellency. Finally, the electrical properties of different coatings including voltage resistance, resistivity, dielectric constant and dielectric loss were characterized, and the mechanism of electrical performance improvement was revealed. This multifunctional superhydrophobic coating is demonstrated to be a candidate for magnesium alloys in complex and harsh environment.

## 2. Experiment

### 2.1. Materials

The AZ31 magnesium alloys (2.5–3.0 wt.% Al, 0.70–1.3 wt.% Zn, 0.2 wt.% Mn, and balanced Mg) used as matrix materials were polished with silicon carbide paper followed

by ultrasonic cleaning in deionized water and ethanol. Silicon dioxide ( $\text{SiO}_2$ ) powder (purity = 99.9%) with a diameter of around 40nm was purchased from Dongguan XinWeiJin Industry Co., Ltd. (Dongguan, China) PTFE resin was purchased from Daikin Industries. All other chemicals including KH-570 silane coupling agent (Hangzhou Jiexika Industry Co., Ltd., Hangzhou, China), and butyl acetate solution (Henan Weiyuan Biotechnology Co., Ltd., Kaifeng, China) were analytical grade reagents.

### 2.2. Preparation of the Superhydrophobic Coating

The superhydrophobic coating was prepared by the following process: First, the mixed solution of  $\text{SiO}_2$ , KH-570 silane coupling agent and ethanol precursors with a mass ratio of 1:1:5 was mechanically stirred for 1 h, then centrifuged at 8000 rpm for 3 min to obtain modified hydrophobic silica particles. Subsequently, mix the hydrophobic nano-silica particles (0, 1 and 3 g) with butyl acetate solution and ultrasonically disperse for 1 h to prepare a dispersion. Then, the PTFE resin (10 g) was slowly added to the dispersion, with magnetic stirring at 1000 r/min for 60 min to ensure that the resin and the solvent dispersion were thoroughly mixed. Finally, the modified PTFE suspension was defoamed in a vacuum dryer (30 °C) for 5 min to obtain a slurry. The slurry is brushed onto the magnesium alloy substrate with subsequent room temperature curing for 5 h to prepare different samples. For convenience, the samples prepared by adding different concentrations (0, 10 wt%, 30 wt%) of silica were called as PTFE, PTFE + 10% $\text{SiO}_2$  and PTFE + 30% $\text{SiO}_2$ , respectively.

### 2.3. Characterization

The surface morphologies and chemical composition of the prepared coating were tested by a scanning electron microscope (SEM, MERLIN Compact, Jena, Germany) and equipped energy dispersive spectroscopy (EDS, MERLIN Compact, Jena, Germany) detector. Water contact angles were measured by a contact angle meter (Attension Theta, Biolin, Sweden), testing at least five different points on each sample, using 5  $\mu\text{L}$  deionized water.

### 2.4. Robust Superhydrophobicity Test

The mechanical durability was measured by linear abrasion with silicon carbide sandpapers (Standard glasspaper, P#600 grit, Zhenxin sandpaper co., Ltd., Wuxi, China). The coating surface was abraded (abrasion distance is 20 cm and circulation of 40 times) by the sandpaper under a weight at 100 g. The thermal shock test was conducted by muffle furnace, and a high temperature of 80 °C for 5 h and a room temperature of 25 °C for 5 h are set as a cycle. The superhydrophobic coating was left outside for 60 days, and the static contact angle was measured for each 10-day period. Additionally, the superhydrophobic coating was exposed to ultraviolet radiation, salt spray corrosion aging room, and sodium chloride solution to further test its environmental stability. Among them, four fluorescent test lamps were hung side by side in the ultraviolet test room, and the coated samples were placed 15 cm away from the lamps. The samples were tilted 30° relative to the horizontal plane to ensure that UV rays were evenly spread across all parts of the sample. In a salt-spray corrosion aging chamber, samples were placed at a level of 45°. After the test, the samples were washed repeatedly with DI water until the salt spray residue attached to the coated surface was washed off. The wettability of the superhydrophobic surface was characterized by droplet impact experiments, which was recorded by a high-speed camera and water droplet dropped from a pre-determined height of 20 mm. The self-cleaning abilities were measured on the superhydrophobic coating by ink,  $\text{MnO}$  powder and dust.

### 2.5. Corrosion Resistance Test

Electrochemical measurements to assess corrosion resistance were performed in a 3.5 wt% NaCl aqueous solutions using a Gamry 600 (Ref. 600, Gamry, Warminster, PA, USA) electrochemical workstation. Electrochemical measurements were performed using a conventional three-electrode configuration, where the specimen was used as working electrode, a saturated calomel electrode (SCE) was used as reference electrode and a platinum

plate was used as the counter electrode. The corrosion resistance test at room temperature. A stable open-circuit potential (OCP) within 600 s was allowed before potentiodynamic polarization test. The scanning rate of the dynamic measurement of polarization curves was 1 mV/s. In order to ensure the reliability of the measurement results, three dynamic potential polarization measurements were carried out for each sample.

### 2.6. Dielectric Performance Tests

Withstanding voltage tester (C-9 series) (Nanjing Instrument Factory, Nanjing, China) was used to test the dielectric strength of the coatings. The electrical resistance was measured by high resistance meter (CHT810 series, Hope Tech, Wuxi, China). The relative permittivity  $\epsilon$  and loss angle tangent  $\tan\delta$  of different coating materials were tested at working frequency using a solid insulation material dielectric loss tester (Beijing IC Times Instrument Equipment Co. LTD, Beijing, China).

## 3. Results and Discussion

### 3.1. Surface Morphology and Wettability

Surface micro/nano morphologies and wettability of different coatings surface with different  $\text{SiO}_2$  loading levels are shown in Figure 1. It can be observed that micron-sized particles are aggregates of the nano- $\text{SiO}_2$  with strong interaction, forming hierarchical micro/nano rough structures on the surface of the coating. As shown in Figure 1a, the PTFE layer homogeneously covers the Mg alloy substrate, forming an even and dense organic layer. Moreover, the dense and defect-free composite layers are also observed after doping with 10wt% and 30wt% nanoparticles (Figure 1b,c). The microscale papillae formed by the aggregation of nanoparticles are adhered together by PTFE, and the surface is covered with nanoparticles. The micro- and nanoscale hierarchical structure traps enough air to prevent water droplets from penetrating into the cavity, thus imparting superhydrophobicity to the surface ( $\text{CA} \approx 170.5^\circ$ , shown in Figure 1d). Additionally, according to static water CA measurements (Figure 1d), the PTFE and PTFE + 10% $\text{SiO}_2$  surfaces are hydrophobic that have water contact angles of  $99.7^\circ$  and  $135.2^\circ$  separately.

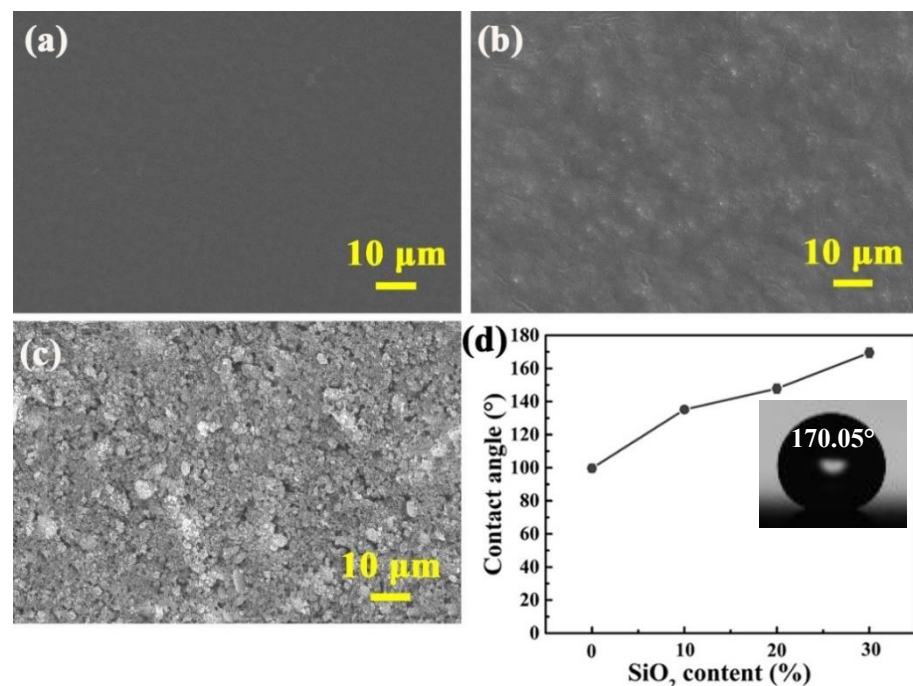


**Figure 1.** Surface micro-topography and contact angle change of (a) PTFE, (b) PTFE + 10% $\text{SiO}_2$  and (c) PTFE + 30% $\text{SiO}_2$ . (d) Variation of contact angle with particle addition.

### 3.2. Corrosion Resistance

The potentiodynamic polarization curves of various samples are shown in Figure 2. The values of the parameters obtained by the Tafel extrapolation method and the protection efficiency  $\eta$  obtained by the equation [36] are listed in Table 1.

$$\eta\% = \frac{I_{corr}^0 - I_{corr}^1}{I_{corr}^0} \times 100\% \quad (1)$$

where  $I_{corr}^1$  and  $I_{corr}^0$  are the  $I_{corr}$  of bare magnesium and other coatings. As depicted in Figure 2 and Table 1, compared with magnesium substrate ( $-1.483$ ), the  $E_{corr}$  of the composite coatings obviously moves to the positive corrosion potential by about  $0.226$  V. The  $I_{corr}$  values of the PTFE and PTFE + 10%SiO<sub>2</sub> coatings are three orders of magnitude lower than that of bare magnesium ( $3.47 \times 10^{-5}$  A cm<sup>-2</sup>), reaching  $7.89 \times 10^{-8}$  and  $7.66 \times 10^{-8}$  A cm<sup>-2</sup>, respectively. The corrosion inhibition efficiency ( $\eta$ ) of PTFE and PTFE + 10%SiO<sub>2</sub> coatings on magnesium alloy substrate is 97.69% and 97.79%, respectively, which further proves that the composite coating has a good corrosion inhibition effect. Compared with PTFE, the  $E_{corr}$  becomes more and more positive and the  $I_{corr}$  becomes smaller as the SiO<sub>2</sub> content increases. Especially for the PTFE + 30%SiO<sub>2</sub> coating is more effective in terms of corrosion protection, which is due to the generated superhydrophobic nanocomposite layer that hinders the diffusion of water and other corrosive substances dissolved in water, such as Cl<sup>-</sup>.

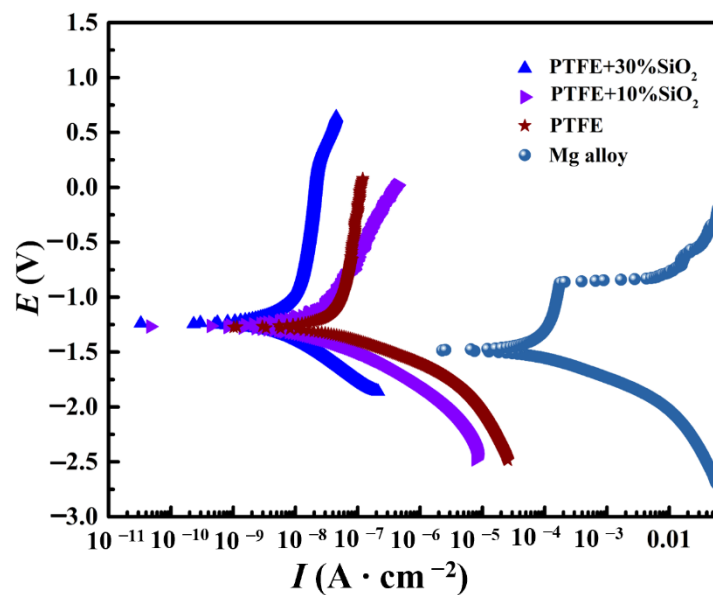


**Figure 2.** Potentiodynamic polarization curves of AZ31 Mg, PTFE, PTFE + 10%SiO<sub>2</sub> and PTFE + 30%SiO<sub>2</sub> coated samples.

**Table 1.** The corresponding parameters of the PDP curves of AZ31 alloy, PTFE + 10%SiO<sub>2</sub> and PTFE + 30%SiO<sub>2</sub> coated samples.

Sample	$E_{corr}$ (V)	$I_{corr}$ (A · cm <sup>-2</sup> )	$R_p$ (Ω · cm <sup>-2</sup> )	$\eta$
AZ31 Mg	-1.483	$3.47 \times 10^{-5}$	1098.52	-
PTFE	-1.293	$7.89 \times 10^{-8}$	$5.84 \times 10^5$	97.69%
PTFE + 10%SiO <sub>2</sub>	-1.257	$7.66 \times 10^{-8}$	$5.99 \times 10^5$	97.79%
PTFE + 30%SiO <sub>2</sub>	-1.229	$3.39 \times 10^{-8}$	$1.20 \times 10^6$	99.02%

### 3.3. Environmental Suitability

Environmental stability is a key to superhydrophobic surfaces that are difficult to overcome due to the inherent fragility of the hierarchical structure that is easily disrupted by

fickle settings [37–39]. Then, to test the wetting stability of the coating, the PTFE + 30%SiO<sub>2</sub> coatings are exposed to harsh and complicated conditions (Figure 3). The results show that the PTFE + 30%SiO<sub>2</sub> coating has a static contact angle greater than 150° after 60 days of exposure to the outdoors (Figure 3a). Due to the PTFE coating with wear-resistant nanoparticles and anti-wear hierarchical morphology, the contact angle is still greater than 150° after 40 abrasion cycles (Figure 3b), which demonstrates the durable superhydrophobicity of the coating. Due to the PTFE coating with wear-resistant nano particles and anti-wear hierarchical morphology, the contact angle is still greater than 150° after 40 abrasion cycles (Figure 3b), which demonstrates the durable superhydrophobicity of the coating. Li et al. [40] reported that the superhydrophobic coating prepared by electrodeposition of cobalt on the AZ31 magnesium alloy surface maintained good mechanical stability and the contact angle decreased by 6° (it decreased from 156.2° ± 0.60° to nearly 150° after 9 m wear of 800# sandpaper). Shi et al. [41] found that the WCA of polyphenylene sulfide-polytetrafluoroethylene/silicon dioxide (4 g/L) coating remained 142.5° after wear of 10 m, and had good wear resistance. Liang et al. [42] reported that the 7.3 wt.% SiO<sub>2</sub>@PTFE coating surface placed facedown to 400 grits SiC sandpaper under load of 5.4 kPa could maintain superhydrophobicity after being rubbed 30 times. The comparison shows that that the PTFE + 30%SiO<sub>2</sub> coating in this work has better wear resistance. The coating remains superhydrophobic after prolonged exposure to salt spray for 150 h (Figure 3c), showing a relatively good chemical stability. The water resistance of super water-repellent coating remains unchanged after thermal shock cycle (>400 h) (Figure 3d). Zang et al. [43] found that the superhydrophobic coating remains superhydrophobic through 18 cycles at high temperature (350 °C). Xie et al. [44] reposted that the PDMS/SiO<sub>2</sub> superhydrophobic coatings can withstand atmospheric temperatures up to 350 °C and has good thermal stability between room temperature (25 °C) and 350 °C. To sum up, the superhydrophobic coating in this work has temperature cycling resistance. The coating shows good UV resistance when exposed to UV radiation for a long time and the contact angle is still greater than 150° (Figure 3e). Figure 3f shows that the contact angles between aqueous droplets with pH value from 1 to 13 and PTFE + 30%SiO<sub>2</sub> coating remain above 160°.

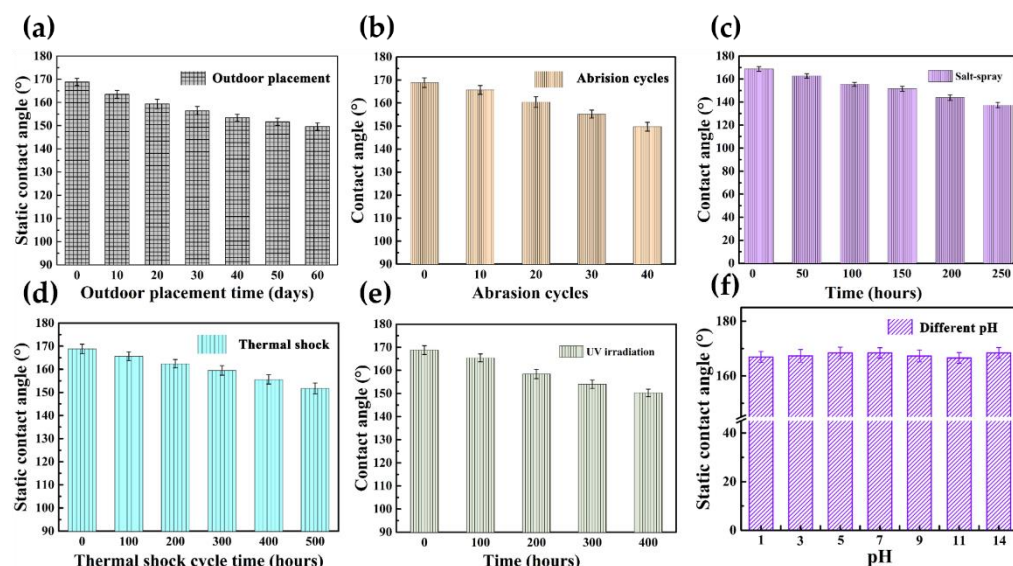


**Figure 3.** CAs of the PTFE + 30%SiO<sub>2</sub> super water-repellent coating under different conditions: (a) outdoor placement, (b) abrasion, (c) salt-spray, NaCl solution, (d) thermal shock cycles, (e) UV irradiation, (f) Statistics of the CAs for the coatings with different pH value droplets.

Additionally, self-cleaning experiments are performed by removing ink, MnO powder and dust on the superhydrophobic surface (Figure 4). The ink droplets roll off the water-repellent coating surface without wetting the surface (Figure 4a). Clean water was doped on a surface randomly scattered with MnO powder and dust (Figure 4b,c). Figure 4b3,c3 show

that the MnO powder and dust have been removed from the surface with no ‘leftovers’ observed on the water-repellent coating surface. Undoubtedly, such robust superhydrophobicity and excellent self-cleaning effect are of great significance in matrix protection and practical application in a complex environment.

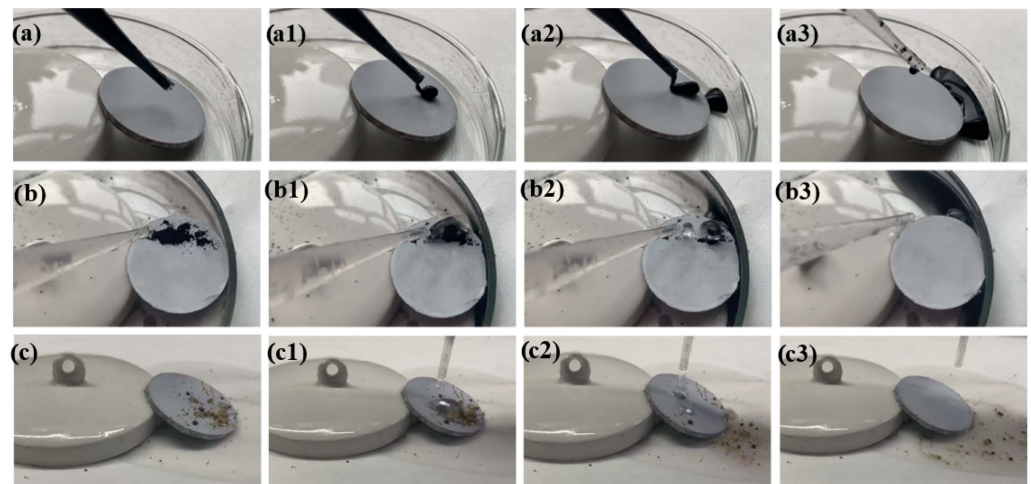


**Figure 4.** Self-cleaning ability of superhydrophobic coating: (a) ink; (b) MnO powder; (c) dust. Self-cleaning process (a1–a3); Self-cleaning MnO powder process (b1–b3); Self-cleaning dust process (c1–c3).

In addition, the water droplets bouncing tests exhibit that water droplets leave the surface completely without wetting the surfaces (Figure 5) and the rebound height is 4.2 mm, which indicates that the surface is water repellent. Therefore, the water-repellent coating has the advantages of small sliding angle, low droplet adhesion and good self-cleaning ability.

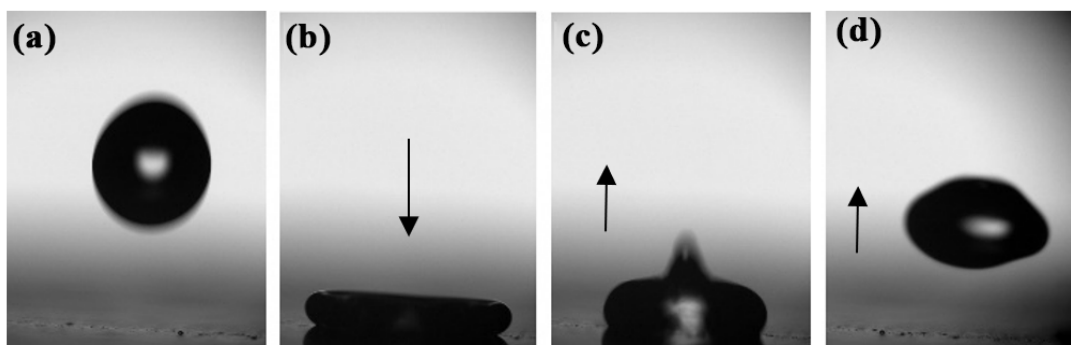


**Figure 5.** Time-lapse photographs of water droplets bouncing on the PTFE + 30%SiO<sub>2</sub> superhydrophobic coating (Droplet sizes of 5  $\mu$ L). (a) Droplets falling, (b) The droplets fall and make contact with the coating, (c) Droplets bounce and (d) The droplets spring up and leave the coating.

### 3.4. Dielectric Properties

The development of superhydrophobic coatings is severely limited due to monotonous functions, especially the electrical properties of superhydrophobic materials are underutilized. Hence, the electric insulation of various coatings is measured and presented in Figure 6. The breakdown voltage of the coatings decreases from 1369.7 V to 1254.5 V with the increase of SiO<sub>2</sub> addition, accompanied by the dielectric strength declines from 36.1 V/ $\mu$ m to 33.8 V/ $\mu$ m (Figure 6a). Obviously, with the increase of SiO<sub>2</sub>, the breakdown strength of the material decreases, due to agglomeration of silicon dioxide fillers, which can destroy the dielectric strength of the coatings [45]. Nevertheless, the dielectric strength of all the organic nanocomposite coatings is obviously higher than 30 V/ $\mu$ m, which is the

result of the wider band gap of polyflon layer at room temperature [46]. The resistivity of the composite coatings can reach  $10^{12} \Omega \cdot \text{cm}$  (Figure 6b), which can be explained by electric insulating PTFE layer that hinders the electron transition.

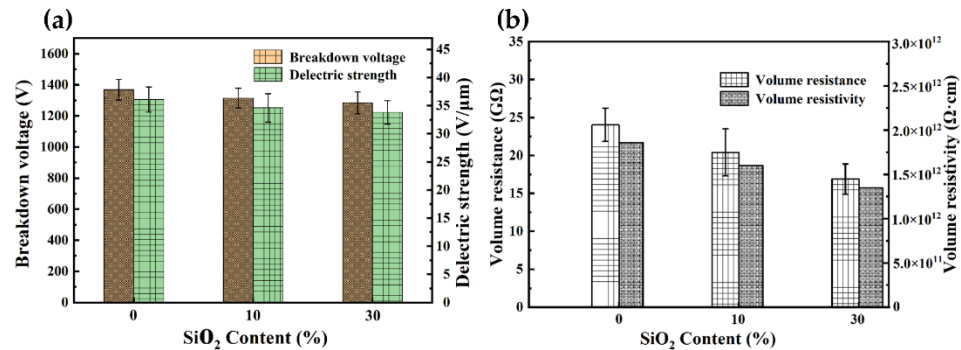


Figure 6. The voltage resistance (a) and electrical resistance properties (b) of various coatings.

In addition, dielectric properties are one of the main properties to be measured for radome materials, which are usually characterized by two indices of dielectric constant ( $\epsilon$ ) and loss angle tangent ( $\tan\delta$ ). For the coating material covering the radome surface, it is important to keep the overall dielectric properties of the radome system without significant fluctuations while reducing the influence of the radome by the external atmospheric environment, to ensure the transmission rate of electromagnetic waves and to reduce the distortion of electromagnetic waves.

Figure 7 shows the effect of silica nanoparticle content on the dielectric constant  $\epsilon$  and loss angle tangent  $\tan\delta$  of the composite coating. The results show that  $\epsilon$  is as low as 3.40 without the addition of silica nanoparticles, indicating that the modified PTFE resin matrix has a significant effect on the enhancement of wave-transparent properties. With the addition of silica nanoparticles, the  $\epsilon$  value increased to 3.91 (PTFE + 30%SiO<sub>2</sub> coating), which may be related to the aggregation caused by the uneven dispersion of silica nanoparticles in the resin due to their low content, and the reflection of electromagnetic waves by this uneven aggregation, thus increasing the  $\epsilon$  value. It can be speculated that the addition of silica nanoparticles has a small enhancement on the electrical properties of the coating, but the inhomogeneous dispersion may reduce its dielectric properties.

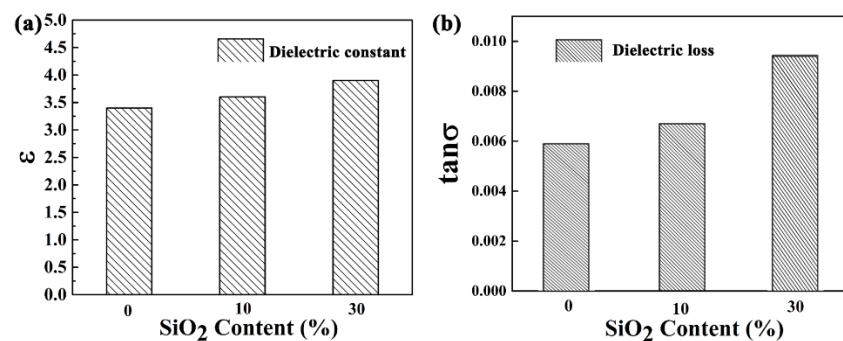


Figure 7. Dielectric constant (a) and dielectric loss (b) of various coatings.

As with  $\epsilon$ , the  $\tan\delta$  of the composite coated test sheets is also low. The dielectric loss increases slightly in the test frequency range with increasing nanoparticle content.  $\tan\delta$  fluctuations may be caused by the diffuse reflection of electromagnetic waves on the irregular nanostructures of the coating surface. The combined results of  $\epsilon$  and  $\tan\delta$  show that the composite coating has good dielectric properties. It can be seen that the PTFE + 30%SiO<sub>2</sub> coating not only has both strong superhydrophobicity and good dielectric properties with dielectric constant ( $\epsilon$ ) of 3.91 and dielectric loss ( $\tan\delta$ ) of 0.0094, indicating that dielectric coatings have great advantages for electronic device protection applications.

Integration of multiple electrical properties, corrosion resistance and robust superhydrophobicity will broaden the innovative application for magnesium alloys in complex and harsh environment, such as electronic equipment and satellite antenna.

#### 4. Conclusions

In summary, a versatile super-repellent coating on the magnesium alloy with robust wettability and design manipulation, based on the integration of organic layer and inorganic nanoparticles hybrid structures was prepared. Thanks to the PTFE layer with wear-resistant nanoparticles and solid hierarchical surface texture, the superhydrophobic coating presents outstanding thermal cycling stability, environmental stability (>60 days), mechanical durability (>40 cycles) and self-cleaning ability. Moreover, the organic composite coating can evenly and densely cover the magnesium alloys, blocking the way for corrosive components to diffuse to the substrate, so that the coating has good corrosion resistance. More importantly, the composite coatings display excellent electrical properties with high dielectric withstanding voltage (>30 V/ $\mu\text{m}$ ) and resistivity (> $10^{12}$   $\Omega\cdot\text{cm}$ ), as well the coating has a low dielectric constant ( $\approx 3.91$ ) and dielectric loss (0.0094), which are great advantage for the electronic or electrical engineering application. The versatile super-repellent coating is promising to be used candidates for novel advanced energy materials, especially in harsh environments.

**Author Contributions:** Conceptualization, W.S.; Data curation, X.B.; Formal analysis, W.S.; Funding acquisition, C.W.; Investigation, Q.K. and C.W.; Methodology, Q.K. and X.B. All authors have read and agreed to the published version of the manuscript.

**Funding:** This research received no external funding.

**Institutional Review Board Statement:** Not applicable.

**Informed Consent Statement:** Not applicable.

**Data Availability Statement:** The authors confirm that the data supporting the findings of this study are available within the article.

**Acknowledgments:** The authors gratefully acknowledge materials and tooling supports for this work from Samcien, Brewer science, AZ electronic materials and HANS laser.

**Conflicts of Interest:** The authors declare no conflict of interest.

#### References

1. Yan, L.K.; Hou, Y.X. The optimization strategies and application of transmission network in power system. *Electric Power Info. Commun. Technol.* **2017**, *107*–112.
2. Kaneto, K. Carrier transports in organic materials related to functional nanometric interface controlled electronic (NICE) devices. *Thin Solid Film.* **2001**, *393*, 249–258. [[CrossRef](#)]
3. Gao, Y.; MacKenzie, R.C.I.; Liu, Y.; Xu, B.; van Loosdrecht, P.H.M.; Tian, W. Organic Electronics: Engineering Ultra Long Charge Carrier Lifetimes in Organic Electronic Devices at Room Temperature. *Adv. Mater. Interfaces* **2015**, *2*, 1400555. [[CrossRef](#)]
4. Lin, C.H.; Huang, C.M.; Wong, T.I.; Chang, H.C.; Juang, T.Y.; Su, W.C. High-Tg and low-dielectric epoxy thermosets based on a propargyl ether-containing phosphinated benzoxazine. *J. Polym. Sci. Polym. Chem.* **2014**, *52*, 1359–1367. [[CrossRef](#)]
5. Lei, Y.; Wang, Q.; Huo, J. Fabrication of durable superhydrophobic coatings with hierarchical structure on inorganic radome materials. *Ceram. Int.* **2014**, *40*, 10907–10914. [[CrossRef](#)]
6. Zhang, R.F.; Zhang, S.F. Formation of micro-arc oxidation coatings on AZ91HP magnesium alloys. *Corros. Sci.* **2009**, *51*, 2820–2825. [[CrossRef](#)]
7. Yu, S.; Jia, R.L.; Zhang, T.; Wang, F.H.; Hou, J.; Zhang, H.X. Effect of Different Scale Precipitates on Corrosion Behavior of Mg-10Gd-3Y-0.4Zr Alloy. *Acta Metall. Sin. Engl.* **2019**, *32*, 433–442. [[CrossRef](#)]
8. Wu, Y.F.; Wang, Y.M.; Jing, Y.B.; Zhuang, J.P.; Yan, J.L.; Shao, Z.K.; Jin, M.S.; Wu, C.J.; Zhou, Y. In vivo study of microarc oxidation coated biodegradable magnesium plate to heal bone fracture defect of 3 mm width. *Colloid Surf. B* **2017**, *158*, 147–156. [[CrossRef](#)]
9. Wu, Y.; Wang, Y.; Tian, S.; Jing, Y.; Zhuang, J.; Guo, L.; Jia, D.; Zhou, Y. Hydrothermal fabrication of rGO/Apatite layers on AZ31 magnesium alloy for enhanced bonding strength and corrosion resistance. *Appl. Surf. Sci.* **2019**, *470*, 430–438. [[CrossRef](#)]
10. Wang, S.Q.; Wang, Y.M.; Chen, J.C.; Zou, Y.C.; Ouyang, J.H.; Jia, D.C.; Zhou, Y. Simple and scalable synthesis of super-repellent multilayer nanocomposite coating on Mg alloy with mechanochemical robustness, high-temperature endurance and electric protection. *J. Magnes. Alloy.* **2022**, *10*, 2446–2459. [[CrossRef](#)]

11. Xu, W.J.; Song, J.L.; Sun, J.; Lu, Y.; Yu, Z.Y. Rapid Fabrication of Large-Area, Corrosion-Resistant Superhydrophobic Mg Alloy Surfaces. *ACS Appl. Mater. Interfaces* **2011**, *3*, 4404–4414. [[CrossRef](#)] [[PubMed](#)]
12. Boinovich, L.; Emelyanenko, A.M.; Modestov, A.D.; Domantovsky, A.G.; Emelyanenko, K.A. Synergistic effect of superhydrophobicity and oxidized layers on corrosion resistance of aluminum alloy surface textured by nanosecond laser treatment. *ACS Appl. Mater. Interfaces* **2015**, *7*, 150813132712001. [[CrossRef](#)] [[PubMed](#)]
13. Boinovich, L.B.; Emelyanenko, A.M.; Modestov, A.D.; Domantovsky, A.G.; Shiryaev, A.A.; Emelyanenko, K.A.; Dvoretzkaya, O.V.; Ganne, A.A. Corrosion behavior of superhydrophobic aluminum alloy in concentrated potassium halide solutions: When the specific anion effect is manifested. *Corros. Sci.* **2016**, *112*, 517–527. [[CrossRef](#)]
14. Li, L.; Huang, T.; Lei, J.; He, J.; Qu, L.; Huang, P.; Zhou, W.; Li, N.; Pan, F. Robust biomimetic-structural superhydrophobic surface on aluminum alloy. *ACS Appl. Mater. Interfaces* **2015**, *7*, 1449–1457. [[CrossRef](#)]
15. Narayanan, T.S.N.S.; Park, I.S.; Lee, M.H. Strategies to improve the corrosion resistance of microarc oxidation (MAO) coated magnesium alloys for degradable implants: Prospects and challenges. *Prog. Mater. Sci.* **2014**, *60*, 1–71. [[CrossRef](#)]
16. Gu, X.N.; Li, N.; Zhou, W.R.; Zheng, Y.F.; Zhao, X.; Cai, Q.Z.; Ruan, L.Q. Corrosion resistance and surface biocompatibility of a microarc oxidation coating on a Mg-Ca alloy. *Acta Biomater.* **2011**, *7*, 1880–1889. [[CrossRef](#)]
17. Wu, Y.F.; Wang, Y.M.; Zhao, D.W.; Zhang, N.; Li, H.Y.; Li, J.L.; Wang, Y.X.; Zhao, Y.; Yan, J.L.; Zhou, Y. In vivo study of microarc oxidation coated Mg alloy as a substitute for bone defect repairing: Degradation behavior, mechanical properties, and bone response. *Colloid Surf. B* **2019**, *181*, 349–359. [[CrossRef](#)]
18. Wang, Y.M.; Wang, F.H.; Xu, M.J.; Zhao, B.; Guo, L.X.; Ouyang, J.H. Microstructure and corrosion behavior of coated AZ91 alloy by microarc oxidation for biomedical application. *Appl. Surf. Sci.* **2009**, *255*, 9124–9131. [[CrossRef](#)]
19. Wu, Y.F.; Wang, Y.M.; Liu, H.; Liu, Y.; Guo, L.X.; Jia, D.C.; Ouyang, J.H.; Zhou, Y. The fabrication and hydrophobic property of micro-nano patterned surface on magnesium alloy using combined sparking sculpture and etching route. *Appl. Surf. Sci.* **2016**, *389*, 80–87. [[CrossRef](#)]
20. Wang, H.Y.; Wei, Y.H.; Liang, M.M.; Hou, L.F.; Li, Y.G.; Guo, C.L. Fabrication of stable and corrosion-resisted super-hydrophobic film on Mg alloy. *Colloid Surf. A* **2016**, *509*, 351–358. [[CrossRef](#)]
21. Saji, V.S. Recent progress in superhydrophobic and superamphiphobic coatings for magnesium and its alloys. *J. Magnes. Alloy* **2021**, *9*, 748–778. [[CrossRef](#)]
22. Liang, M.M.; Wei, Y.H.; Hou, L.F.; Wang, H.Y.; Li, Y.G.; Guo, C.L. Fabrication of a super-hydrophobic surface on a magnesium alloy by a simple method. *J. Alloys Compd.* **2016**, *656*, 311–317. [[CrossRef](#)]
23. Tian, X.; Verho, T.; Ras, R.H.A. Moving superhydrophobic surfaces toward real-world applications. *Science* **2016**, *352*, 142–143. [[CrossRef](#)] [[PubMed](#)]
24. Yao, W.H.; Wu, L.; Huang, G.S.; Jiang, B.; Atrens, A.; Pan, F.S. Superhydrophobic coatings for corrosion protection of magnesium alloys. *J. Mater. Sci. Technol.* **2020**, *52*, 100–118. [[CrossRef](#)]
25. Wang, S.Q.; Wang, Y.M.; Zou, Y.C.; Chen, G.L.; Ouyang, J.H.; Jia, D.C.; Zhou, Y. Scalable-Manufactured Superhydrophobic Multilayer Nanocomposite Coating with Mechanochemical Robustness and High-Temperature Endurance. *ACS Appl. Mater. Interfaces* **2020**, *12*, 35502–35512. [[CrossRef](#)]
26. Seongmin, K.; Jae, H.H.; Handong, C.; Dukhyun, C.; Woonbong, H. Repeatable replication method with liquid infiltration to fabricate robust, flexible, and transparent, anti-reflective superhydrophobic polymer films on a large scale. *Chem. Eng. J.* **2018**, *350*, 225–232.
27. Ou, J.; Hu, W.; Xue, M.; Wang, F.; Li, W. Superhydrophobic surfaces on light alloy substrates fabricated by a versatile process and their corrosion protection. *ACS Appl. Mater. Interfaces* **2013**, *5*, 3101–3107. [[CrossRef](#)]
28. Long, M.; Peng, S.; Deng, W.; Yang, X.; Deng, W. Robust and thermal-healing superhydrophobic surfaces by spin-coating of polydimethylsiloxane. *J. Colloid Interface Sci.* **2017**, *508*, 18. [[CrossRef](#)]
29. Wang, S.; Wang, Y.; Cao, G.; Chen, J.; Zou, Y.; Yang, B.; Ouyang, J.; Jia, D.; Zhou, Y. Highly reliable double-layer coatings on magnesium alloy surfaces for robust superhydrophobicity, chemical durability and electrical property. *Ceram. Int.* **2021**, *47*, 35037–35047. [[CrossRef](#)]
30. Lu, S.; Chen, Y.; Xu, W.; Wei, L. Controlled growth of superhydrophobic films by sol-gel method on aluminum substrate. *Appl. Surf. Sci.* **2010**, *256*, 6072–6075. [[CrossRef](#)]
31. Zhang, F.Z.; Zhao, L.L.; Chen, H.; Xu, S.; Evans, D.G.; Duan, X. Corrosion Resistance of Superhydrophobic Layered Double Hydroxide Films on Aluminum. *Acta Metal. Sin.* **2008**, *47*, 2466–2469.
32. Liu, Y.; Liu, J.; Li, S.; Liu, J.; Han, Z.; Ren, L. Biomimetic Superhydrophobic Surface of High Adhesion Fabricated with Micronano Binary Structure on Aluminum Alloy. *ACS Appl. Mater. Interfaces* **2013**, *5*, 8907–8914. [[CrossRef](#)] [[PubMed](#)]
33. Xu, N.; Sarkar, D.K.; Chen, X.G.; Tong, W.P. Corrosion performance of superhydrophobic nickel stearate/nickel hydroxide thin films on aluminum alloy by a simple one-step electrodeposition process. *Surf. Coat. Technol.* **2016**, *302*, 173–184. [[CrossRef](#)]
34. Kannarpady, G.K.; Khedir, K.R.; Ishihara, H.; Woo, J.; Oshin, O.D.; Trigwell, S.; Ryerson, C.; Biris, A.S. Controlled Growth of Self-Organized Hexagonal Arrays of Metallic Nanorods Using Template-Assisted Glancing Angle Deposition for Superhydrophobic Applications. *ACS Appl. Mater. Interfaces* **2011**, *3*, 2332–2340. [[CrossRef](#)] [[PubMed](#)]
35. Wang, S.Q.; Wang, Y.M.; Zou, Y.C.; Wu, Y.F.; Chen, G.L.; Ouyang, J.H.; Jia, D.C.; Zhou, Y. A self-adjusting PTFE/TiO<sub>2</sub> hydrophobic double-layer coating for corrosion resistance and electrical insulation. *Chem. Eng. J.* **2020**, *402*, 126116. [[CrossRef](#)]

36. Zhu, H.Z.; Yue, L.F.; Zhuang, C. Fabrication and characterization of self-assembled graphene oxide/silane coatings for corrosion resistance. *Surf. Coating. Technol.* **2016**, *304*, 76–84. [[CrossRef](#)]
37. Wang, S.Q.; Wang, Y.M.; Zhang, H.J.; Zhou, Y.C.; Chen, G.L.; Ouyang, J.H.; Jia, D.C.; Zhou, Y. Co-growing design of super-repellent dual-layer coating for multiple heat dissipation improvement. *Chem. Eng. J.* **2022**, *427*, 131701. [[CrossRef](#)]
38. Liu, M.L.; Luo, Y.F.; Jia, D.M. A Robust and Versatile Continuous Super-Repellent Polymeric Film for Easy Repair and Underwater Display. *ACS Appl. Mater. Interfaces* **2020**, *12*, 6677–6687. [[CrossRef](#)]
39. Peng, C.Y.; Chen, Z.Y.; Tiwari, M.K. All-organic superhydrophobic coatings with mechanochemical robustness and liquid impalement resistance. *Nat. Mater.* **2018**, *17*, 355–360. [[CrossRef](#)]
40. Li, W.; Kang, Z. Fabrication of corrosion resistant superhydrophobic surface with self-cleaning property on magnesium alloy and its mechanical stability. *Surf. Coatings Technol.* **2014**, *253*, 205–213. [[CrossRef](#)]
41. Shi, L.; Hu, J.; Lin, X.D.; Fang, L.; Wu, F.; Xie, J.; Meng, F.M. A robust superhydrophobic PPS-PTFE/SiO<sub>2</sub> composite coating on AZ31 Mg alloy with excellent wear and corrosion resistance properties. *J. Alloys Compd.* **2017**, *721*, 157–163. [[CrossRef](#)]
42. Liang, Y.; Ju, J.; Deng, N. Super-hydrophobic self-cleaning bead-like SiO<sub>2</sub>@ PTFE nanofiber membranes for waterproof-breathable applications. *Appl. Surf. Sci.* **2018**, *442*, 54–64. [[CrossRef](#)]
43. Zang, D.M.; Zhu, R.W.; Zhang, W.; Yu, X.Q.; Lin, L.; Guo, X.L.; Liu, M.J.; Jiang, L. Corrosion-Resistant Superhydrophobic Coatings on Mg Alloy Surfaces Inspired by Lotus Seedpod. *Adv. Funct. Mater.* **2017**, *27*, 1605446. [[CrossRef](#)]
44. Xie, J.; Hu, J.; Lin, X. Robust and anti-corrosive PDMS/SiO<sub>2</sub> superhydrophobic coatings fabricated on magnesium alloys with different-sized SiO<sub>2</sub> nanoparticles. *Appl. Surf. Sci.* **2018**, *457*, 870–880. [[CrossRef](#)]
45. Li, H.Y.; Liu, G.; Liu, B.; Chen, W.; Chen, S.T. Dielectric properties of polyimide Al<sub>2</sub>O<sub>3</sub> hybrids synthesized by in-situ polymerization. *Mater. Lett.* **2007**, *61*, 1507–1511. [[CrossRef](#)]
46. Yang, D.; Huang, S.; Ruan, M.N.; Li, S.X.; Yang, J.W.; Wu, Y.B.; Guo, W.L.; Zhang, L.Q. Mussel Inspired Modification for Aluminum Oxide/Silicone Elastomer Composites with Largely Improved Thermal Conductivity and Low Dielectric Constant. *Ind. Eng. Chem. Res.* **2018**, *57*, 3255–3262. [[CrossRef](#)]